Journal of Theoretical and Applied Mechanics, Sofia, Vol.51 (2021) pp. 407-420
SOLID MECHANICS

DELAMINATION CRACK STUDY OF A MULTILAYERED INHOMOGENEOUS BEAM EXHIBITING STRESS RELAXATION

VICTOR RIZOV*

Department of Technical Mechanics, University of Architecture, Civil Engineering and Geodesy, 1 Chr. Smirnensky blvd, 1046-Sofia, Bulgaria

[Received: 30 March 2020. Accepted: 05 April 2021]

ABSTRACT: The present article is concerned with a delamination crack analysis of a multi-layered inhomogeneous cantilever beam that exhibits stress relaxation. A linear viscoelastic model consisting of two springs and a dashpot is used for treating the stress relaxation. The moduli of elasticity of the springs and the coefficient of viscosity of the dashpot vary continuously along the thickness of each layer. A time-dependent solution to the strain energy release rate that accounts for the stress relaxation is derived. The J-integral approach is a in order to verify the solution to the strain energy release rate. The solution is applied to evaluate the stress relaxation induced variation of the strain energy release rate in the multi-layered cantilever beam with the time.

KEY WORDS: Multi-layered beam, Inhomogeneous layers, Stress relaxation, Delamination crack.

1 INTRODUCTION

Inhomogeneous structural materials with continuously changing mechanical properties in the solid are frequently used in various load-bearing applications in nowadays engineering. One of the most important features of these materials is the fact that their properties are continuous functions of the coordinates. It should be mentioned that one of continuously inhomogeneous materials which are currently receiving notable attention in the specialized literature is the functionally graded materials [1–7]. This is due mainly to the fact that the properties of the functionally graded materials can be formed technologically during the manufacturing process in order to satisfy different exploitation requirements in different parts of a structural member. The functionally graded materials find applications as advanced structural materials in important structures in aeronautical engineering, nuclear power plants, piezoelectric and thermoelectric devices, automotive industry, biomedicine and others.

The engineering practice indicates that one of the principal causes for failure of many inhomogeneous structural members and components is the appearance of

*Corresponding author e-mail: v_rizov_fhe@uacg.bg

cracks. The reliability and durability of continuously inhomogeneous load-bearing structures depend manly on their fracture behaviour. Therefore, the significance of fracture analyses of inhomogeneous materials and structures is well recognized by the research community [8–12].

Various aspects of the problem of fracture analysis of continuously inhomogeneous structural materials have been considered in [8]. It has been shown that fracture in continuously inhomogeneous materials and structures can be analysed successfully by applying methods of linear-elastic fracture mechanics. Different fracture problems of functionally graded materials have been addressed and approaches for their solution have been developed. The debonding of coatings made of functionally graded materials has also been investigated and discussed.

A review of various fracture studies of functionally graded composite materials has been presented in [9]. Fracture behaviour under static or fatigue cyclic crack loading conditions has been analysed. Solutions to different crack problems in structural materials with graded composition have been considered. Cracks oriented parallel or perpendicular to the material gradient direction have been studied by using methods of linear-elastic fracture mechanics. Investigations of straight-linear and circular arch cracks have been discussed.

Cracks in functionally graded materials and structures have been analysed in [10]. For this purpose, methods of linear-elastic fracture mechanics have been used. An engineering approach for predicting the strength of functionally graded structures containing cracks has been developed. The approach has been applied for beams and plates made of functionally graded materials.

The present paper deals with analysis of the strain energy release rate for a delamination crack in a multi-layered inhomogeneous cantilever beam that exhibits stress relaxation. The paper is motivated by the fact that inhomogeneous (functionally graded) materials and structural components often have viscoelastic behaviour [13–16]. Therefore, an adequate analysis of a time-dependent delamination in a beam structure should take into account the viscoelastic behaviour. It should be mentioned that fracture analyses of functionally graded viscoelastic materials are focussed mainly on central cracks in infinitely long strips or in half-planes [17, 18]. Also, the analyses presented in [17, 18] are concerned with deriving of time-dependent solutions of the stress intensity factors. In contrast to [17, 18], a time-dependent solution of the strain energy release rate in a beam configuration is derived here. A linear viscoelastic model is applied for describing the stress-relaxation behaviour in the present paper. The solution is applied to evaluate the stress relaxation induced variation of the strain energy release rate with the time. The effects of continuous variation of the modulii of elasticity and the coefficients of viscosity along the thickness of the beam layers on the strain energy release rate are evaluated too.

2 Analysis of the Strain Energy Release Rate

A multi-layered inhomogeneous cantilever beam is shown schematically in Fig. 1. The beam consists of adhesively bonded horizontal layers. The number of layers is arbitrary. The layers have different thickness and material properties. Each layer exhibits continuous material inhomogeneity in the thickness direction. The beam is clamped in its right-hand end. The cross-section of the beam is a rectangle of width b and thickness h. The length of the beam is l. A delamination crack of length a is located arbitrary between layers. The thicknesses of the lower and the upper delamination crack arms are denoted by h_1 and h_2, respectively. The free end of the lower delamination crack arm is quickly loaded in pure bending and then held so as the strains in the beam remain constant with the time. The angle of rotation of the free end of the lower delamination crack arm is denoted by ϕ (Fig. 1). The upper delamination crack arm is free of stresses. While the strains remain constant, the stresses in the beam decrease with the time, i.e. the beam exhibits stress relaxation. In the present paper, a solution to the strain energy release rate is derived by using the linear viscoelastic model under constant applied strain shown in Fig. 2. The viscoelastic model of the i-th layer of the beam consists of two linear springs of modulii of elasticity, E_{1i} and E_{2i}, and a linear dashpot of coefficient of viscosity, η_i. The variation of the stress, σ_i, in the i-th layer of the beam with the time, t, is written as [19]:

$$\sigma_i = E_{0i}\varepsilon + (E_{2i} - E_{0i})\varepsilon e^{-(E_{2i}-E_{0i})t/\eta_i}\,, \tag{1}$$

where:

$$E_{0i} = \frac{E_{2i}E_{1i}}{E_{2i} + E_{1i}}\,. \tag{2}$$

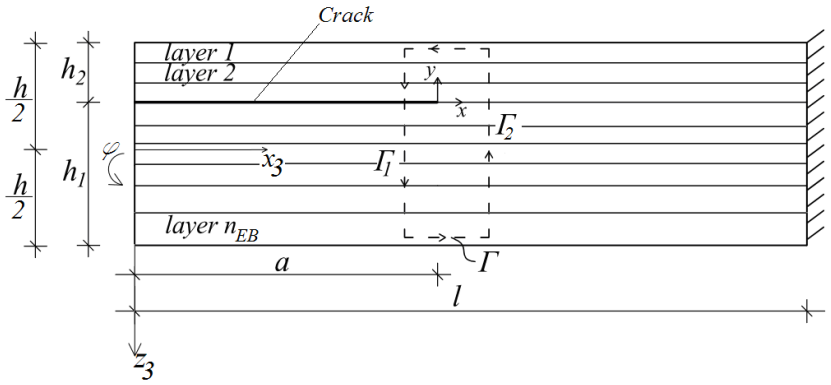

Fig. 1: Multi-layered cantilever beam configuration with a delamination crack.

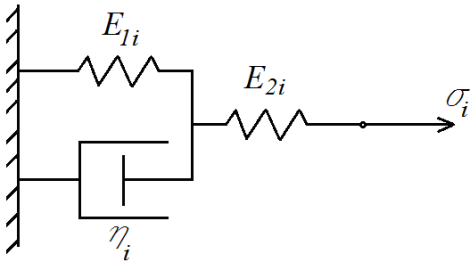

Fig. 2: Linear viscoelastic model with two springs and a dashpot.

In formula (1), ε is the strain. Since the layers are continuously inhomogeneous in the thickness direction, the distributions of E_{1i}, E_{2i}, and η_i along the thickness of the i-th layer are expressed as:

$$E_{1i} = E_{1iU} + \frac{E_{1iU} - E_{1iL}}{(z_{3i} - z_{3i+1})^{m_i}}(z_{3i} - z_3)^{m_i}\,, \tag{3}$$

$$E_{2i} = E_{2iU} + \frac{E_{2iU} - E_{2iL}}{(z_{3i} - z_{3i+1})^{s_i}}(z_{3i} - z_3)^{s_i}\,, \tag{4}$$

$$\eta_i = \eta_{iU} + \frac{\eta_{iU} - \eta_{iL}}{(z_{3i} - z_{3i+1})^{f_i}}(z_{3i} - z_3)^{f_i}\,, \tag{5}$$

where

$$z_{3i} \leq z_3 \leq z_{3i+1}\,. \tag{6}$$

In formulae (3)–(5), E_{1iU}, E_{2iU}, and η_{iU} are, respectively, the values of E_{1i}, E_{2i}, and η_i in the upper surface of the i-th layer, the values of E_{1i}, E_{2i}, and η_i in the lower surface of the same layer are denoted, respectively, by E_{1iL}, E_{2iL}, and η_{iL}, the material properties, m_i, s_i, and f_i, control the distributions, respectively, of E_{1i}, E_{2i}, and η_i along the thickness of the layer, z_3 is the vertical centroidal axis of the beam, z_{3i} and z_{3i+1} are the coordinates, respectively, of the upper and lower surface of the layer under consideration.

The strain energy release rate, G, for the delamination crack in the multi-layered beam configuration shown in Fig. 1 is obtained by differentiating the strain energy, U, in the beam with respect to the delamination crack area

$$G = \frac{dU}{bda}\,, \tag{7}$$

where da is an elementary increase of the delamination crack length.

Since the upper delamination crack is free of stresses, the strain energy cumulated in the multi-layered beam is obtained as

$$U = U_{LW} + U_{EB}\,, \tag{8}$$

where U_{LW} and U_{EB} are the strain energies, respectively, in the lower delamination crack arm and in the un-cracked beam portion, $a \leq x_3 \leq l$, where x_3 is the longitudinal centroidal axis of the beam (Fig. 1).

The strain energy cumulated in the lower delamination crack arm is expressed as

$$U_{LW} = a \sum_{i=1}^{i=n_{LW}} \iint\limits_{(A_i)} u_{0LWi} dA\,, \tag{9}$$

where n_{LW} is the number of layers in the same crack arm (Fig. 3), u_{0LWi} is the strain energy density in the i-th layer, A_i is the area of the cross-section of the layer.

The strain energy density is found as

$$u_{0LWi} = \frac{1}{2}\sigma_i \varepsilon\,. \tag{10}$$

By combining of (1) in (10), one obtains the following time-dependent expression

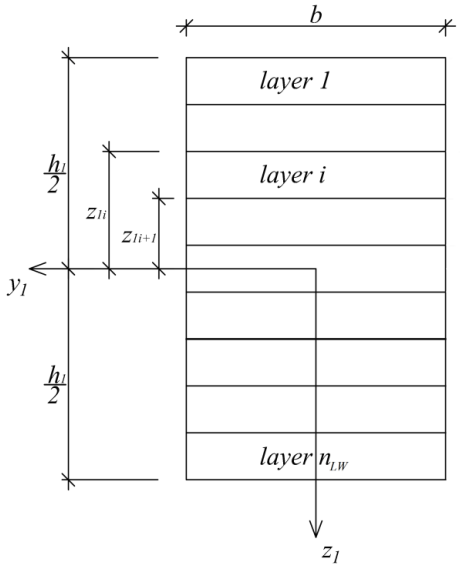

Fig. 3: Cross-section of the lower delamination crack arm.

for the strain energy density:

$$u_{0LWi} = \frac{1}{2}\left[E_{0i}\varepsilon^2 + (E_{2i} - E_{0i})\varepsilon^2 e^{-(E_{2i}-E_{0i})t/\eta_i}\right]. \tag{11}$$

In the present article, the strains are treated by applying the Bernoulli's hypothesis for plane sections, since the beam under consideration has high length to thickness ratio. Therefore, the distribution of the strains along the thickness of the lower delamination crack arm is expressed as:

$$\varepsilon = \kappa_{LW}(z_1 - z_{1n}), \tag{12}$$

where

$$-\frac{h_1}{2} \leq z_1 \leq \frac{h_1}{2}. \tag{13}$$

In formula (12), κ_{LW} is the curvature of the lower crack arm, z_1 is the vertical centroidal axis of the cross-section of the crack arm, z_{1n} is the coordinate of the neutral axis. It should be noted that the neutral axis shifts from the centroid since the beam under consideration is multi-layered and inhomogeneous.

The curvatures and the coordinates of the neutral axis of the lower delamination crack arm and the un-cracked beam portion are determined by using four equations which are composed in the following manner. First, since the beam is loaded in pure bending, the axial force in the lower delamination crack arm is zero

$$\sum_{i=1}^{i=n_{LW}} \iint\limits_{(A_i)} \sigma_i dA = 0, \tag{14}$$

where the distribution of σ_i along the thickness of the i-th layer is found by substituting of (12) in (1).

Analogically, the axial force in the un-cracked beam portion is also zero

$$\sum_{i=1}^{i=n_{EB}} \iint\limits_{(A_i)} \sigma_{EBi} dA = 0, \tag{15}$$

where n_{EB} is the number of layers in the un-cracked beam portion, σ_{EBi} is the stress in the i-th layer of the un-cracked beam portion. The stress, σ_{EBi}, is found by using formula (1). For this purpose, ε is replaced with ε_{EB}. The distribution of the strain, ε_{EB}, along the thickness of the un-cracked beam portion is written as

$$\varepsilon_{EB} = \kappa_{EB}(z_2 - z_{2n}), \tag{16}$$

where

$$-\frac{h}{2} \leq z_2 \leq \frac{h}{2}\,. \tag{17}$$

In formula (16), κ_{EB} is the curvature of the un-cracked beam portion, z_2 is the vertical centroidal axis of the cross-section of the un-cracked beam portion, z_{2n} is the coordinate of the neutral axis. The distribution of σ_{EBi} along the thickness of the i-th layer in the un-cracked beam portion is obtained by substituting of (16) in (1).

A further one equation is written by using the fact the bending moments in the lower delamination crack arm and in the un-cracked beam portion are equal

$$\sum_{i=1}^{i=n_{LW}} \iint\limits_{(A_i)} \sigma_i z_1 dA = \sum_{i=1}^{i=n_{EB}} \iint\limits_{(A_i)} \sigma_{EBi} z_2 dA = 0\,. \tag{18}$$

Finally, one equation is composed by expressing the angle of rotation of the free end of the lower delamination crack arm as a function of the curvatures of the lower crack arm and the un-cracked beam portion. For this purpose, the integrals of Maxwell-Mohr are applied. The result is

$$\phi = \kappa_{LW} a + \kappa_{EB}(l-a)\,. \tag{19}$$

After substituting of σ_i and σ_{EBi} in (14), (15), (18) and (19), the four equations are solved with respect to κ_{LW}, z_{1n}, κ_{EB} and z_{2n} at various values of time by using the MATLAB program.

The strain energy cumulated in the un-cracked beam portion is written as

$$U_{EB} = (l-a) \sum_{i=1}^{i=n_{EB}} \iint\limits_{(A_i)} u_{0EBi} dA\,, \tag{20}$$

where u_{0EBi} is the strain energy density in the i-th layer, A_i is the area of the cross-section of the same layer. Formula (11) is applied to calculate u_{0EBi}. For this purpose, ε is replaced with ε_{EB}.

After substituting of (9) and (20) in (7), one obtains the following solution to the strain energy release rate:

$$G = \frac{1}{b}\left(\sum_{i=1}^{i=n_{LW}} \iint\limits_{(A_i)} u_{0LWi} dA - \sum_{i=1}^{i=n_{EB}} \iint\limits_{(A_i)} u_{0EBi} dA \right). \tag{21}$$

The integration in (21) is carried-out by using the MATLAB program. It should be mentioned that solution (21) is time-dependent since the strain energy densities are functions of the time according to (11). This fact indicates that (21) can be used to evaluate the variation of the strain energy release rate with the time due to the stress relaxation.

The J-integral approach is applied in order to verify the time-dependent solution to the strain energy release rate [20]. The J-integral is solved along the integration contour, Γ, shown by a dashed line in Fig. 1. The upper delamination crack arm is free of stresses. Therefore, the J-integral solution is written as

$$J = J_{\Gamma_1} + J_{\Gamma_2}\,, \tag{22}$$

where J_{Γ_1} and J_{Γ_2} are, respectively, the values of the J-integral in segments, Γ_1 and Γ_2, of the integration contour (segments, Γ_1 and Γ_2, coincide with the cross-sections of the lower delamination crack arm and the un-cracked beam portion, respectively).

The J-integral in segment, Γ_1, is written as

$$J_{\Gamma_1} = \sum_{i=1}^{n_{LW}} \int_{z_{1i}}^{z_{1i+1}} \left[u_{0LWi} \cos\alpha - \left(p_{xi} \frac{\partial u}{\partial x} + p_{yi} \frac{\partial v}{\partial x} \right) \right] ds\,, \tag{23}$$

where z_{1i} and z_{1i+1} are the coordinates, respectively, of the upper and lower surface of the i-th layer in the lower delamination crack arm (Fig. 3), α is the angle between the outwards normal vector to the contour of integration and the delamination crack direction, p_{xi} and p_{yi} are the stress vector components in the i-th layer, u and v are the components of displacement vector with respect to the crack tip coordinate system xy, ds is a differential element along the integration contour.

The components of (23) are written as

$$p_{xi} = -\sigma_i\,, \tag{24}$$

$$p_{yi} = 0\,, \tag{25}$$

$$ds = dz_1\,, \tag{26}$$

$$\cos\alpha = -1\,, \tag{27}$$

$$\frac{\partial u}{\partial x} = \varepsilon\,, \tag{28}$$

where ε is calculated by (12).

In segment, Γ_2, the J-integral is expressed as

$$J_{\Gamma_2} = \sum_{i=1}^{n_{EB}} \int_{z_{2i}}^{z_{2i+1}} \left[u_{0EBi} \cos\alpha_{EB} - \left(p_{xi_{EB}} \frac{\partial u}{\partial x_{EB}} + p_{yi_{EB}} \frac{\partial v}{\partial x}_{EB} \right) \right] ds_{EB}\,, \tag{29}$$

where z_{2i} and z_{2i+1} are the coordinates, respectively, of the upper and lower surface of the i-th layer in the un-cracked beam portion. The other components of J_{Γ_2} are obtained as

$$p_{xi_{EB}} = \sigma_{EBi}\,, \tag{30}$$

$$p_{yi_{EB}} = 0\,, \tag{31}$$

$$ds_{EB} = -dz_2\,, \tag{32}$$

$$\cos\alpha_{EB} = 1\,, \tag{33}$$

$$\frac{\partial u}{\partial x_{EB}} = \varepsilon_{EB}\,. \tag{34}$$

The strain, ε_{EB}, that is involved in (34) is found by (16).
After substituting of (23) and (29) in (22), one obtains

$$J = \sum_{i=1}^{n_{LW}} \int_{z_{1i}}^{z_{1i+1}} \left[u_{0LWi}\cos\alpha - \left(p_{xi}\frac{\partial u}{\partial x} + p_{yi}\frac{\partial v}{\partial x} \right) \right] ds + \sum_{i=1}^{n_{EB}} \int_{z_{2i}}^{z_{2i+1}} \left[u_{0EBi}\cos\alpha_{EB} - \left(p_{xi_{EB}}\frac{\partial u}{\partial x_{EB}} + p_{yi_{EB}}\frac{\partial v}{\partial x}_{EB} \right) \right] ds_{EB}\,. \tag{35}$$

The MATLAB computer program is used to perform the integration in (35). The fact that the J-integral value calculated by (35) is equal to the strain energy release rate obtained by (21) is a verification of the analysis developed in the present paper. It should be noted that the solution (35) can be used to calculate the J-integral at various values of the time since the strain energy densities are continuous functions of t (refer to formula (11)).

3 Numerical Results

The results presented in this section of the paper illustrate the stress relaxation induced variation of the strain energy release rate with the time and the effects of material inhomogeneity in the layers of the multi-layered beam on the strain energy release rate. For this purpose, the time-dependent solution to the strain energy release rate (21) is applied. The strain energy release rate is presented in non-dimensional form by using the formula $G_N = G/(E_{11U}b)$. In order to evaluate the effect of the delamination crack location along the thickness of the cantilever beam on the time-dependent strain energy release rate, two three-layered beam configurations are analysed (Fig. 4). The thickness of each layer in both beam configurations is h_t. In the beam configuration shown in Fig. 4a, a delamination crack of length, a, is located

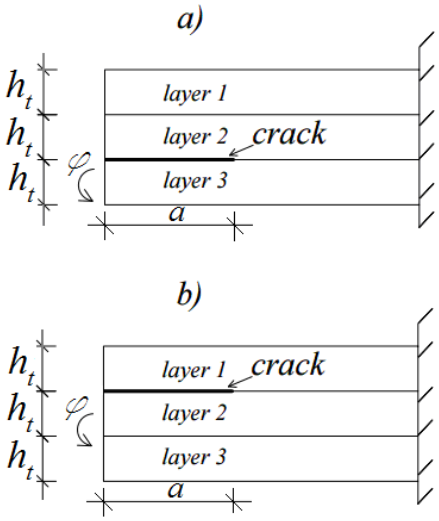

Fig. 4: Two three-layered cantilever beam configurations with a delamination crack (a) located between layers 2 and 3, and (b) located between layers 1 and 2.

between layers 2 and 3. A delamination crack between layers 1 and 2 is also analysed (Fig. 4b). It is assumed that $l = 0.3$ m, $a = 0.15$ m, $h_t = 0.002$ m, $b = 0.008$ m, $\phi = 0.005$ rad, $m_i = 0.7$, $s_i = 0.7$ and $f_i = 0.7$ where $i = 1,\ 2,\ 3$.

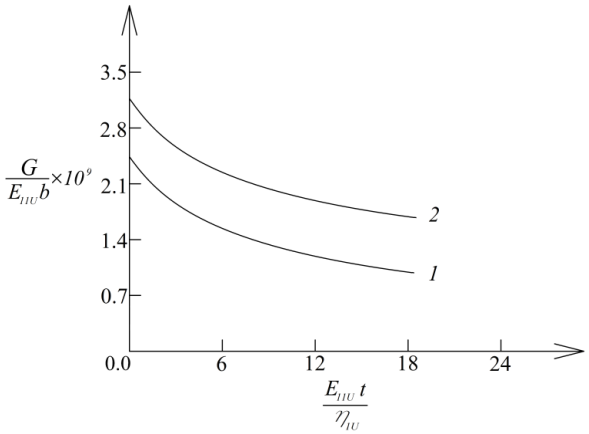

Fig. 5: The strain energy release rate in non-dimensional form plotted against the non-dimensional time (curve 1 – for delamination crack located between layers 1 and 2, curve 2 – for delamination crack located between layers 2 and 3).

The variation of the strain energy release rate in non-dimensional form with the time is shown in Fig. 5 for both three-layered cantilever beam configurations depicted in Fig. 4. The time in Fig. 5 is expressed in non-dimensional form by using the formula $t_N = tE_{11U}/\eta_{1U}$. The curves in Fig. 5 indicate that the strain energy release rate decreases with the time (this finding is attributed to the stress relaxation). The strain energy release rate at $t = 0$ in Fig. 5 is due to the instantaneous linear-elastic strain modelled by the spring with modulus of elasticity, E_{2i} (Fig. 2). It can also be observed in Fig. 5 that the strain energy release rate in the three-layered cantilever beam configuration with a delamination crack located between layers 2 and 3 is higher than that in the configuration with a delamination crack between layers 1 and 2.

The effects of the continuous variation of modulii of elasticity, E_{11} and E_{21}, along the thickness of layer 1 is examined in Fig. 6 where the strain energy release rate in non-dimensional form is plotted against E_{11L}/E_{11U} ratio at three E_{21L}/E_{21U} ratio. The three-layered cantilever beam configuration with a delamination crack located between layers 2 and 3 is considered. It is evident from Fig. 6 that the strain energy release rate increases with increasing of E_{11L}/E_{11U} and E_{21L}/E_{21U} ratios.

The influence of the continuous variation of the coefficient of viscosity, η_1, in the thickness direction of layer 1 on the strain energy release rate is also investigated. For this purpose, calculations of the strain energy release rate are carried-out at various η_{1L}/η_{1U} ratios. The cantilever beam with a delamination crack between layers 2 and 3 is analysed. The strain energy release rate in non-dimensional form is plotted

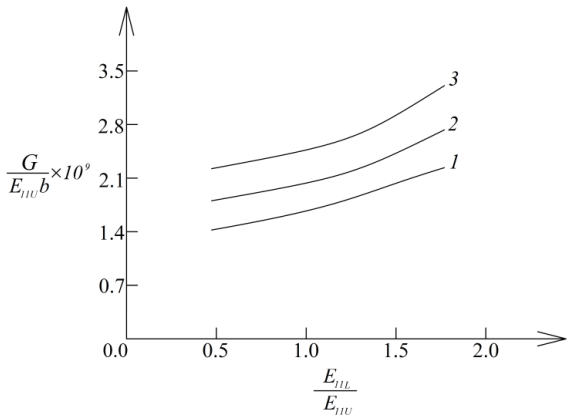

Fig. 6: The strain energy release rate in non-dimensional form plotted against E_{11L}/E_{11U} ratio (curve 1 – at $E_{21L}/E_{21U} = 0.5$, curve 2 – at $E_{21L}/E_{21U} = 1.0$ and curve 3 – at $E_{21L}/E_{21U} = 2.0$).

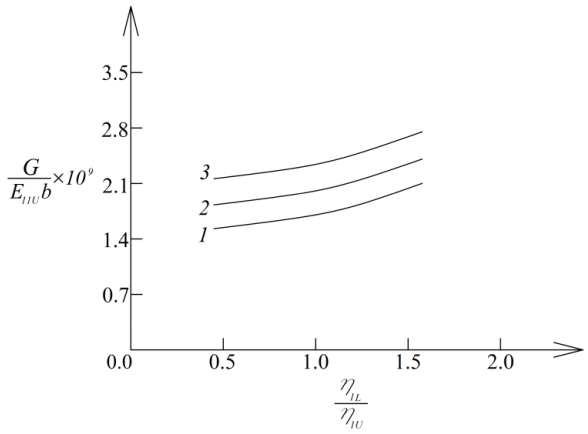

Fig. 7: The strain energy release rate in non-dimensional form plotted against η_{1L}/η_{1U} ratio (curve 1 – at $\phi = 0.003$ rad, curve 2 – at $\phi = 0.004$ rad and curve 3 – at $\phi = 0.005$ rad).

against η_{1L}/η_{1U} ratio in Fig. 7 at three values of ϕ. It can be observed in Fig. 7 that the strain energy release rate increases with increasing of η_{1L}/η_{1U} ratio. The curve in Fig. 7 show that the strain energy release rate increases with increasing of ϕ.

4 Conclusions

The influence of the stress relaxation on the strain energy release rate for a delamination crack in a multi-layered inhomogeneous cantilever beam configuration is analysed. For this purpose, a time-dependent solution to the strain energy release rate is derived. The beam under consideration is made of adhesively bonded layers. The delamination crack is located arbitrary between layers. Thus, the thicknesses of the lower and the upper delamination crack arms are different. The number of layers is arbitrary. Each layer has individual thickness and material properties. The material in the layers is continuously inhomogeneous in the thickness direction. The layers exhibit stress relaxation that is treated by using a linear viscoelastic model which consists of two springs and a dashpot. The moduli of elasticity of the springs and the coefficient of viscosity of the dashpot vary continuously in the thickness direction of the layers. The time-dependent solution to the strain energy release rate is obtained by differentiating the strain energy cumulated in the multi-layered beam with respect to the delamination crack area. The curvatures and the coordinates of the neutral axis of the lower delamination crack arm and the un-cracked beam portion which are used when deriving the time-dependent solution to the strain energy release rate are obtained by considering the equilibrium of the lower delamination crack arm and the

un-cracked beam portion. A time-dependent solution to the J-integral is derived in order to verify the strain energy release rate. The variation of the strain energy release rate with the time due to stress relaxation is analysed. It is found that the strain energy release rate decreases with the time as a result of the stress relaxation. The effect of the delamination crack location along the beam thickness is analysed too. The analysis reveals that the strain energy release rate decreases with increasing the thickness of the lower delamination crack arm. The influence of the material inhomogeneity on the time-dependent strain energy release rate is investigated. The material inhomogeneity is characterized by E_{11L}/E_{11U}, E_{21L}/E_{21U} and η_{1L}/η_{1U} ratios. It is found that the strain energy release rate increases with increasing of E_{11L}/E_{11U}, E_{21L}/E_{21U} and η_{1L}/η_{1U} ratios.

REFERENCES

[1] M. KOIZUMI (1993) The concept of FGM Ceramic Trans. *Functionally Gradient Materials* **34** 3-10.

[2] A. NEUBRAND, J. RÖDEL (1997) Gradient materials: An overview of a novel concept. *Zeitschrift fur Metallkunde* **88** 358-371.

[3] M. GASIK (2010) Functionally graded materials: bulk processing techniques. *International Journal of Materials and Product Technology* **39** 20-29.

[4] M. NEMAT-ALLAL, M. ATA, M. BAYOUMI, W. KHAIR-ELDEEN (2011) Powder metallurgical fabrication and microstructural investigations of Aluminum/Steel functionally graded material. *Materials Sciences and Applications* **2** 1708-1718.

[5] S. BOHIDAR, R. SHARMA, P. MISHRA (2014) Functionally graded materials: A critical review. *International Journal of Research* **1** 289-301.

[6] M. EL-WAZERY, A. EL-DESOUKY (2015) A review on functionally graded ceramic-metal materials. *Material Environment Science* **6** 1369-1376.

[7] R. MAHAMOOD, E. AKINLABI (2017) Functionally Graded Materials. Springer.

[8] F. ERDOGAN (1995) Fracture mechanics of functionally graded materials. *Computational Engineering* **5** 753-770.

[9] M. TILBROOK, R. MOON, M. HOFFMAN (2005) Crack propagation in graded composites. *Composites Science and Technology* **65** 201-220.

[10] A. CARPINTERI, N. PUGNO (2006) Cracks in re-entrant corners in functionally graded materials. *Engineering Fracture Mechanics* **73** 1279-1291.

[11] V. RIZOV (2019) Analysis of the Strain Energy Release Rate for a Delamination Crack in a Multilayered Beam with Material Non-Linearity. *IOP Conference Series: Materials Science and Engineering* **473** 012002.

[12] V. RIZOV (2020) Inhomogeneous Multilayered Beams of Linearly Changing Width: a Delamination Analysis, *IOP Conference Series: Materials Science and Engineering*. **739** 012004.

[13] W.X. ZHANG, R.G. LIU, G.Y. BAI (2017) Applications of the symplectic method in quasi-static analysis for viscoelastic functionally graded materials. *Engineering Computations* **34** 1314-1331.

[14] H.H. HILTON (2005) Optimum linear and non-linear viscoelastic designer functionally graded materials – characterization and analysis. *Composites Part A: Applied Science and Manufacturing* **36** 1329-1334.

[15] H.H. HILTON, D.H. LEE, A.R.A. EL FOULY (2008) Generalized viscoelastic designer functionally graded auxetic materials engineered/tailored for specific task performances. *Mechanics of Time-Dependent Materials* **12** 1521-1567.

[16] Z.H. JIN (2006) Some Notes on the Linear Viscoelasticity of Functionally Graded Materials. *Mathematics and Mechanics of Solids* **11** 216-224.

[17] WENZHI YANG, ZENGTAO CHEN (2019) Thermo-viscoelastic response of a cracked, functionally graded half-plane under a thermal shock. *Engineering Fracture Mechanics* **206** 267-277.

[18] Z.H. WANG, L. ZHANG, L.C. GUO (2013) Fracture analysis of a viscoelastic functionally graded materials strip with a central crack. *Journal of Physics: Conference Series* **419** 012015.

[19] V. ZUBCHANINOV (1990) Theory of elasticity and plasticity. Vishaia shkola.

[20] D. BROEK (1986) Elementary engineering fracture mechanics. Springer.